Keynote speaker: 3D Stereolithography by Using Two-Photon Photopolymerization

*Ran Hee Kim, Kwang-Sup Lee**

Summary: This article describes the development and evolution of two-photon lithography of 3-dimensional (3D) polymeric structures through two-photon photopolymerization (TPP) and the materials used to facilitate the same. The first part elaborates on the advantages of TPP over conventional lithographic techniques used in the fabrication of 3D microelectromechanical systems (MEMS). The second part introduces the preparation of highly efficient organic two-photon absorbing materials based on the centro-symmetric π-conjugated system and their performance as sensitizers in two-photon polymerization.

Keywords: 3D patterning; TPA photoinitiators; two-photon absorption; two-photon photopolymerization

Introduction

Speed and precision are highly desirable qualities in a lithographic technique employed in 3-dimensional microelectromechanical systems (3D MEMS). Two-photon photopolymeri- zation (TPP) achieves both of these qualities by the application of photopolymerization in the farbication of MEMS.[1] 3D MEMS technology can be virtually devided into time before and after TPP. The conventional 3D MEMS technologies consist of two parts. In the first part 3D target objects are designed using computer-aided design (CAD) and the resulting data is sliced into a series of data sets defining horizontal planes that add up to form the model.[2] The second step involves the transfer of the generated data into photopolymerized areas additively forming the real microstructures through photopoly-merization of photocurable resins. The latter is complicated and time-consuming. During photopolymerization step either continuous wave or pulsed laser systems are employed to induce polymerization. The laser sources in case of two-photon polymerization are pulsed.

In conventional MEMS device fabrication polymerization results from a linear optical absorption. The photocurable resin is exposed to ultraviolet laser scan and solidified in the 2D shape according to one sliceed CAD 3D pattern, over which resin is added as a thin layer. The other 2D sliced pattern is laser-scaned and polymerized on the first layer, and then the same process is continued successively until completing the 3D CAD microstructure. This is called the ''layer by layer'' method. Commercial 3D MEMS process involves lot of time and effort making it an expensive process. Moreover this process places an inherent mechanical limit for fabrication of nanoscale resolution.[3]

TPP's superiority over the commercial 3D microfabrication methods comes from the two-photon absorption (TPA) phenomenon, which is a spatially selective nonlinear optical property. A highly intense light source, namely a laser is required to make TPA possible, which was 1960 that Theodore Maiman invented the first ruby laser.[4] Though originally predicted by Göppert-Meyer in the 1930s,[5] it was observed experimentally only in 1961 when

Department of Advanced Materials Hannam University, 461-1 Junmin-Dong Yusung-Gu, Daejeon 305-811, Republic of Korea
Fax: (+82) 42 629 8870; E-mail: kslee@hnu.kr

Kaiser and Garret demonstated two-photon absorption in CaF_2: Eu^{+2} crystals with a ruby laser.[6] In this article we provide an overview of TPP 3D nano/microfabrication, and the development of organic two-photon absorbing materials with large TPA activities. An effort has been made to describe the detail information on TPP 3D microfabrications and look over diverse strategies to design of highly efficient two-photon absorbing molecules. However, it is well outside the focus of the paper to cover all the methods and materials related to two-photon 3D microfabrication. We have instead focused on the investigation of the centrosymmetric organic two-photon absorbing materials and an illustration of the TPP technologies as a tool for 3D nano/microfabrications.

Two-Photon Photopolymerization

Photopolymerization refers to the chain-growth polymerization employing light to initiate the polymerization. In a radical photopolymerization, the mixture of photoinitiators (or sometimes with photosensitizers) and small molecules called as monomers or oligomers are irradiated by ultraviolet, visible to infrared region radiation. The radiation frequency is determined by the photoinitiator types. The radical photopolymerization consists of four steps; (i) the decomposition of initiators (ii) initiation, (iii) chain propagation, and (iv) the termination step.[7]

In a linear absorption photopolymerization, as the photoinitiator (I) is exposed to the radiation with a suitable frequency, the initiator absorbs a photon, goes to the excited state, and then decomposes into radicals ($R^{\bullet}$) *via* inermediate (I^{*}), called the decomposition step according to the following equations:

$$I \xrightarrow{\hbar\nu} I^{*} \rightarrow R^{\bullet} \quad (1)$$

$$R^{\bullet} + M \xrightarrow{M} RM^{\bullet} \quad (2)$$

$$RM^{\bullet} \xrightarrow{M} RMM^{\bullet} \xrightarrow{M}\xrightarrow{M} \cdots \rightarrow RM_n^{\bullet} \quad (3)$$

$$M_n^{\bullet} + M_m^{\bullet} \rightarrow M_{n+m} \quad (4)$$

$$M_n^{\bullet} + M_m^{\bullet} \rightarrow M_n + M_m \quad (5)$$

where $\hbar$ is the Planck's constant devided by 2π and ν is the radiation frequency, $\hbar\nu$ corresponds to the energy absorbed by an initiator. This photogenerated radical ($R^{\bullet}$) is a reactive species that would further react with monomers or oligomers, which is called the *initiation* step. In the second step, as shown in the equation (2), the resulting radical, $RM^{\bullet}$ transfers to another monomer resulting in new radical, $RMM^{\bullet}$, which undergoes the *chain* reactions up to n monomers forming $RM_n^{\bullet}$, which can be written M_n when n is large number. Whenever the other monomer is combined to the radical, the radical chain grows in several hundred thousands of molecular weight, called the chain *propagation* step. Generally the chain propagation terminates in two paths; i) the long chain radicals meet each other to form M_{n+m} (coupling reaction), as described in the equation (4) or ii) disproportion reaction as in the equation (5).

Sometimes in the photoinitiation stage, a *photosensitizer* (S), is introduced to absorb the light and then transfer the energy to an initiator molecule to go to the excited state. This working process of the photosensitizer can be described as follows:

$$S \xrightarrow{\hbar\nu} S^{*} \rightarrow \xrightarrow{I} I^{*} \rightarrow 2R^{\bullet} \quad (6)$$

As for the characteristics of the final polymers, they can be either linear thermoplastics or crosslinked polymers according to the functionality of monomers or oligomers.[7] In TPP stereolithography, a two-photon chromophore acts as either a photosensitizer that absorbs energy and imparts it to a photoinitiator, or as a photoinitiator which would undergo a photoinduced decomposition to intiate the polymerization reaction.

The difference between one-photon absorption and TPA process are shown in Figure 1. In one-photon absorption, a photon with frequency ν_1 is absorbed and the molecule is excited from ground state S_0 to the first excited state S_1 (Figure 1a).

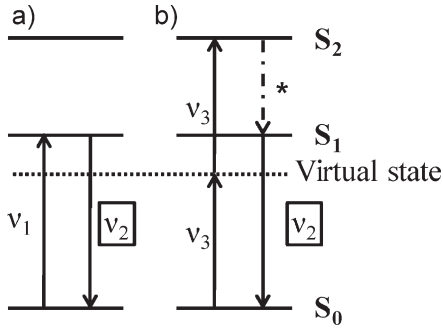

Figure 1.
Schemetic illustration of (a) the one-photon absorption (OPA) and (b) the degenerate two-photon absorption (TPA) processes of a material through a virtual state. * is a nonradiative decay.

However, using the highly intense light source, two photons with the same frequency ν_3 (so it is called degenerate) are simultaneously absorbed to be excited to the two-photon allowed state S_2. This is followed by a nonradiative relaxation to the S_1 state. From S_1 the molecule relaxes to S_0 in a typical radiative decay and emiting a photon, with the same frequency ν_2 (Figure 1b).[8]

TPA response depends quadratically on the intensity of the incident radiation. The result of this dependence is that it occurs only within a confined area near the focus of the beam path. The quadratic dependence of TPA characterics provide highly useful spatial selectivity for TPA phenomena in the case of photopolymerization over the one-photon absorption. First, in order to get the photoinitiator excited, photon in the near infrared (NIR) regime are used. NIR radiation by virtue or its longer wavelength shows high penetrability inside a material allowing the initiation of polymerization within the bulk of a two-photon sensitized photopolymerizable resin. The apparent spatial selectivity of the TPA process limits the damage to the regions of polymerizable media sourrounding the focus. Since the whole exposed regions are absorbing in the UV-Vis region of the spectrum in the case of one-photon absorption there can be considerable lateral damage to the photoactive materials used for one-photon based fabrication. The high spatial selectivity of two-photon absorption allows fabrication of features with sub-wavelength dimensions.[8]

In the last couple of decades, lots of efforts have been made in materials, mechanics and optics to realize 3D nano/microfabrication using TPP. Thanks to these efforts, the optical laser system set up for 3D TPP nanostereolithography is optimized as illustrated in the following Figure 2.[9] As a beam source a mode-locked Ti:Sapphire laser with 80 MHz repetition and short pulse width of less than 100 femtosecond is used. The radiation time is controlled with a Galvano Shutter. The beam is expanded by a lens to increase the accuracy in the beam propagating direction (usually z direction). The position of the focus inside the photopolymerizable material is adjusted with the piezoelectric stage along the z direction. The planar direction (x, y) of the beam is controlled by focusing it on a Galvano mirror scanner.The laser beam goes through the objective lens (numerical aperture of 1.4) and is focused in the position programmed by CAD data and the scanned pattern can be seen real time in the monitor connected to the charge-coupled-device (CCD) camera. Immersion oil is used between the objective lens and the substrate plate on which the oligomers are applied, to reduce the refractive index difference. Finally a fabricated 3D pattern on the glass substrate is isolated by removing the residual oligomers containing TPA photosenstisizers simply with organic solvents. The whole scan proceed continuously in one stage without any further addition of oligomers.

Lots of studies to improve the quality of TPP 3D nanopatterns have been reported.[8,10,11] In this section, some basic issues to determine the resolution of 3D TPP nanostereolithography are discussed. A voxel (*volumetric pixel*) dimension and shape are important to improve the fabrication precision.[12] The voxel is formed by a single exposure of laser beam controlled by Galvano shutter in photocurable oligo-

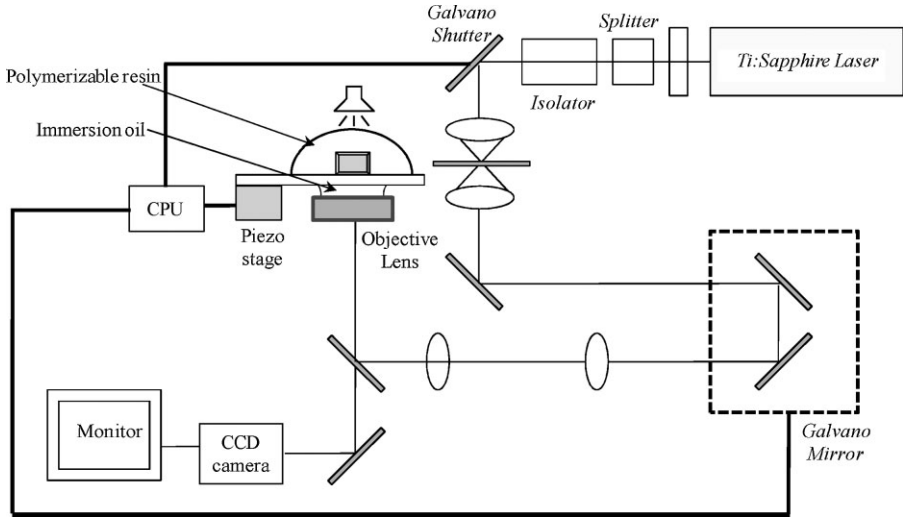

Figure 2.
Laser set up for 3D nanostereolithography using TPP.

mers, having an oval shape. A voxel dimension is tuned dominantly by both exposure time and laser power. A minimum power and minimum exposure time Scheme 3D TPP fabrication was investigated experimentally and theoretically and optimized, by its application of the exposure time of 20 ms and exposure power of 40 mW.[13] Further, for the enhancement of strength of the 3D TPP microstructures, double contour scanning method was proposed. The 3D structures constructed by double contour scanning were found to be stronger than that made by a single contour scanning method (see Figure 3).[14]

In addition the surface smoothness was the drawback to be overcome for the fine microstructures. By applying a novel sub-regional slicing method (SSM) instead of the existing uniform slicing method (USM) in the CAD data especially in a curved region, the micro vase with better smooth surface was successively fabricated and is shown in the Figure 4.[15]

When a 3D photonic crystal (PhC) was fabricated by TPP with an oligomeric acrylic urethane resin (SCR-500), the shringkage of the photonic crystal was found by S. Kawata et. al. As dimension of the microstucture influences the optical

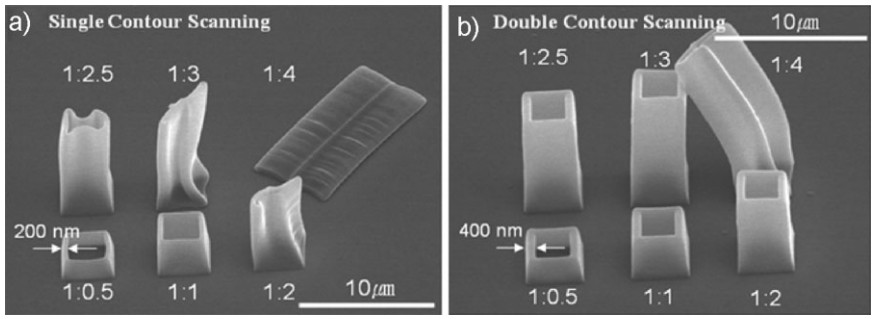

Figure 3.
SEM images of the patterns obtained by (a) single contour scanning and (b) double contour scanning method.

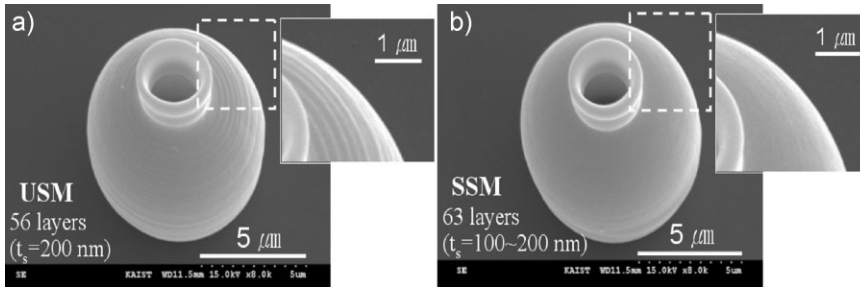

Figure 4.
(A) Scanning electron microscope (SEM) images of the micro base TPP fabricated using the USM and (B). SEM image of the micro base TPP fabricated in SSM. t_s is the slicing thickness in nanometer.

properties in photonic crystals, shrinkage of dimensions is considered highly undesirable for proper operation of photonic crystal fabricated. A shape precompensation technique was proposed to solve the problem.[11] This deformation is caused by the surface tension of the solvent used in the washing process and the lateral shrinkage was found at a rate of 2%/μm. When a 3D desirable object is planned, the shrinkage in size is considered and compensated in advance in the CAD data. The resulting structure is constructed in the size that it is intended.

Recently a novel way to increase the bandgap effect of photonic crystal was reported by the authors. Not only the exact lattice structure of photonic crystal, but also the refractive index of the material play an important role in improving the bandgap effect of photonic crystal. As shown in Figure 5, an acrylic copper compex has introduced to the oligomer and fabricated a 3D woodfile photonic crystal, and succeed in increasing the bandgap upto 34% compared to the photonic crystal TPP fabricated with just photocurable resin (SCR-500) without copper.[16]

Two-Photon Absorbing Chromophores for TPP

Highly efficient organic two-photon absorbing materials have been in great demand due to the widespread study of their application in 3D data storage devices,[17] fluorescence microscopy for 3D bioimaging,[18] optical power limiting,[19] 3D MEMS,[11] up-converted lasing,[20] etc. In 3D MEMS fabrication field the higher the TPA activities, the better resolution can be achieved. Due to their higher reponse to the incident light intensity TPA can occur in a low power of incident light even with continuous wave (CW) lasers and nanosecond lasers. The enormous researches have been performed to improve the TPA activity of organic materials. Investigations in the last couple of decades have led to an understanding of many prominent factors influencing the properties of two-photon absorbing chromophores. Thanks to these efforts we are now in a stage where we can systematically discuss organic two-photon absorbing molecules and aspects of their structure property relationship. TPA active dyes can be classified in four categories by their structures and electric polarity as follows:

(1) Push-pull dipolar TPA dyes
(2) Centrosymmetric quadrupolar TPA dyes
(3) Octupolar and Multi-branched TPA dyes
(4) Polymeric and dendritic TPA dyes.

The schematic representation of their chemical structures is shown in Figure 6. They commonly have π-electron conjuga-

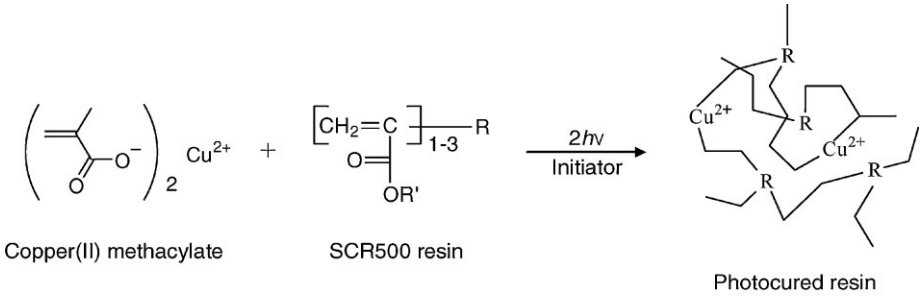

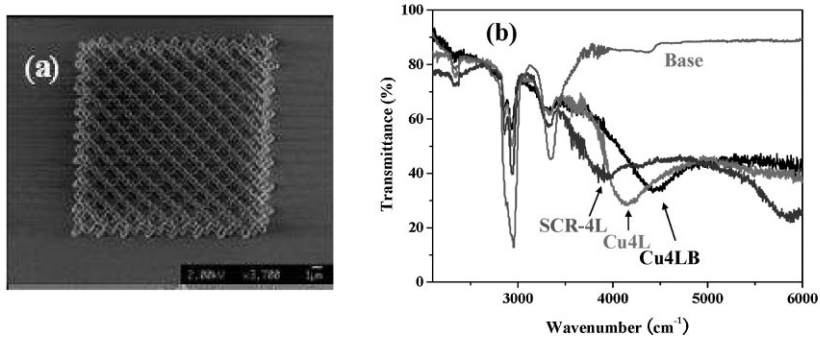

Figure 5.
(a) SEM image of photonic crystal structure fabricated by TPP. (b) FT-IR transmittance spectra of photonic crystals without Cu ion (SCR-4L) and with Cu ion (Cu4L), and Cu4LB after heating at 210 °C for 1 hour and photonic crystal (Cu4L) with the base of UV cured pure resin.

tion and the electron pathways within a molecule. The generic structural design features for efficient TPA dyes include extended π-conjugation, coplanarity throughout the molecular backbone and electronic polarizability for all types of TPA dyes.

In this review we are to concentrate on the centrosymmetric quadrupolar two-photon absorbing chromophores. TPA activity of a material is related with the imaginary part of the third-order optical susceptibility, $\chi^{(3)}_{imag}$, a nonlinear absorption. The measurement of TPA activity of a

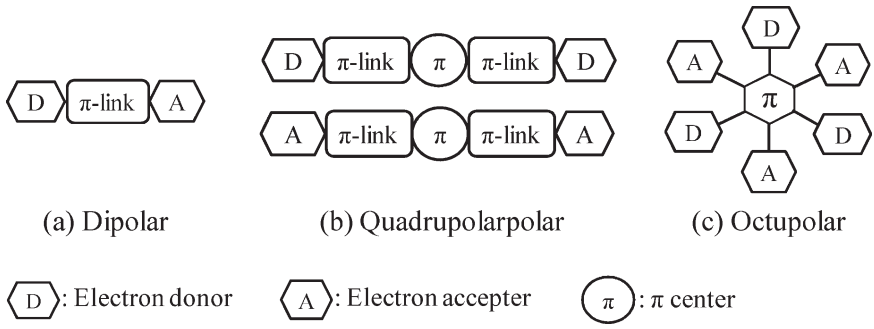

Figure 6.
Schematic simplified illustration of the TPA dyes. In (c) octupolar TPA molecules, " – " corresponds to the π-links.

material is expressed as a TPA cross-section, σ_2, of which unit is Göppert-Meyer (GM, 1 GM = 10^{-50} cm^4 · sec/photon · molecule). A pioneering study by M. Albota and coworkers established the basic factors influencing structure-property relationship in centrosymmetric TPA molecules.[20] The intramolecular charge transfer property is considerably attributed to enhance the TPA activity of the linear molecules. The theoretical explanation for their observations using sum-over-states (SOS) method for TPA cross-section, σ_2 was expressed as following equation, the simplified SOS expression:

$$\sigma_2(s_0 \rightarrow s_2) \propto \frac{M_{01}^2 M_{12}^2}{(E_1 - E_0 - \hbar\omega)\Gamma} \quad (7)$$

where E_n and M_{nm} are the energy state of n and the transition dipole moment between n and m states respectively. The $\hbar\omega$ is the photon energy corresponding to a half of the energy for TPA transition, S_0 to S_2. The parameters in the equation (7) can be tuned to increase σ_2 by modifying the molecular structures so that (E_1 - E_0 - $\hbar\omega$) could decrease and M_{01} and M_{12} increase. It was well known that chain length extension results in an increase in M_{01} and the introduction of donors at the ends or types of π-links leads primarily to an increase in M_{12}. Namely, the TPA properties of a molecule can be managed by the choice of nature π-conjugation of the core and electron donor and/or acceptor strength.

The key molecular structural elements to enhance TPA activity for the design of linear centrosymmetric quadrupolar two-photon absorbing molecules are (i) extension of π-conjugation, (ii) placement of acceptors on the center ring, (iii) increase of donor or accepter strength, and (iv) reversal of the direction of charge transfer as shown in Figure 6(b) like D-π-D to A-π-A.

Two-photon absorbing molecules can be employed as photosensitizers in TPP as mentioned previously in equation (6). Efficiency of TPA molecules plays a key role in improving the precision and resolution of TPP fabrication. When a photosensitizer gets larger TPA cross-section, the less power of laser can be used for TPP fabrication system. This allows a better resolution in TPP leading to reduction of cost and time. For TPP application, the authors have designed and prepared highly efficient centrosymmetric and pseudo-centrosymmetric quadrupolar two-photon absorbing chromophores corresponding to Figure 6(b) based on the structure-property relationship established.[21]

The representitive TPA chromophores are classified according to the type of π-centers: (i) phenylenevinylene and phenyleneethynylene derivatives (**Pa** and **Pc**)[13,22,23] (ii) fluorene derivatives (**Fa** and **Fb**),[24,25] (iii) dithieno[3,2-b;20,30-d]thiophene (DTT) derivatives (**Ta** and **Tc**).[26,27] Their chemical structures and σ_2 values shown in Figure 7. Their TPA cross-section values are measured in two-photon induced fluorescence method using a 80 femtosecond-pulsed laser. TPA activities of some of these chromophores were found to large enough to perform TPP fabrication with good resolution.

In phenylenevinylene and phenyleneethynylene series **Pa** through **Pc** the elongation of molecular backbone influences on the TPA activity. The same is the case in the series of fused thiophene, **Ta** to **Tc**. The introduction of ethynylene moiety as a π-link to a molecule caused the blue-shift of TPA maximum wavelength and solubility problem. More delocalized π-cores such as fluorene and DTT than phenylene exhibited larger TPA activity. Comparing the fluorene and thiophene derivatives, thiophene is a little better than the flourene as a π-core due to the electron rich sulfur element. It is clearly shown that TPA efficiency enhances as the donor strength increases in both case of fluorene and thiophene series. Conclusively the nature of the end group, donor strength and π-delocalization all contribute to the TPA response increase. Optical transparency of the two-photon absorbing chromophores near infrared regime between 680 and 800 nm is essential for their application in TPP nano-stereolithography. In order to avoid linear absorption by the two-photon

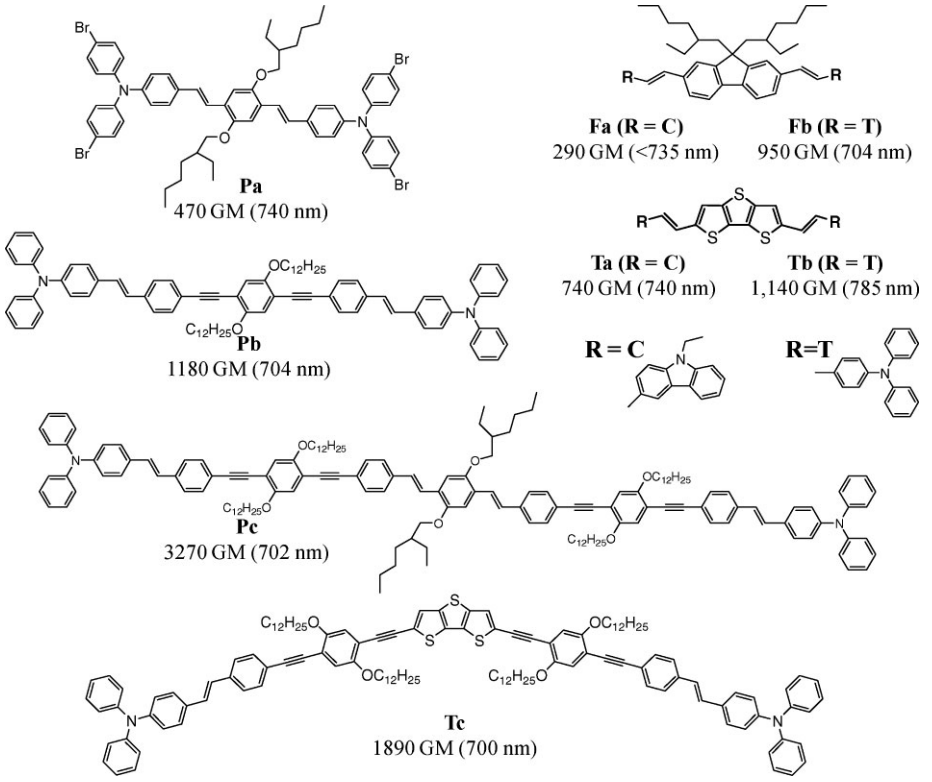

Figure 7.
Chemical structures and the TPA cross-sections (σ_2, GM = 10^{-50} cm^4 · sec/photon· molecule) of centrosymmetric and pseudo-cnetrosymmetric quadrupolar TPA chromophores.

absorbing chromophores during TPP, these chromophores exhibit no absorption above 500 nm.

Conclusion

In the field of 3D MEMS it is a goal to achieve the speed and economy in manufacturing. So far the extensive advances above discussed have been achieved by the continuous efforts and contribution of devoted researcher and scientists in the fields of 3D nano-stereolithography by TPP and TPA materials development. However, the TPP nanofabrication needs further exploration to complete yet. The photocurable oligomeric resins, the strength of fabricated stuctures, and the solubility of the sensitizing two-photon absorbing chromophores are some of the areas where new studies could be made. The research of TPP nano-stereolithography keeps going on and wait the reseachers with a spirit of challenge and creativity.

[1] S. Maruo, O. Nakamura, S. Kawata, *Opt. Lett.* **1997**, 22, 132.
[2] A. Bertsch, H. Lorenz, P. Renaud, Combining microstereolithography and thick resist UV lithography for 3D microfabrication. Proc IEEE MEMS **1998**, 18–23
[3] J. O. Foaussier, "*Photoinitiation, Photopolymerization, and Photocuring: Fundamentals andapplications*", Hanser Publishers, Munich Vienna New York 1995.
[4] T. H. Maiman, *Nature* **1960**, *187*(4736), 493.
[5] M. Göeppert-Mayer, *Ann d Phys.* **1931**, *9*, 273.
[6] W. Kaiser, C. G. B. Garret, *Phys. Rev. Lett.* **1961**, *7*, 229.
[7] G. Odian, "*Principles of Polymerization*", John Wiley & Sons Publication, **2004**.

[8] S. Kawata, H. B. Sun, T. Tanaka, K. Takada, *Nature* **2001**, *412*(16), 697.
[9] K.-S. Lee, R. H. Kim, D.-Y. Yang, S. H. Park, *Polym. Adv. Technol.* **2006**, *17*, 72.
[10] T. Tanaka, H. B. Sun, S. Kawata, *Appl. Phys. Lett.* **2002**, *80*, 312.
[11] H. B. Sun, T. Suwa, K. Takada, R. P. Zaccaria, M. S. Kim, K.-S. Lee, S. Kawata, *Appl. Phys. Lett.* **2004**, *85*(17), 3708.
[12] H. B. Sun, K. Tanaka, S. Kawata, *Appl. Phys. Lett.* **2002**, *80*(20), 3673.
[13] H. B. Sun, K. Takada, M. S. Kim, K.-S. Lee, S. Kawata, *Appl. Phys. Lett.* **2003**, *83*(6), 1104.
[14] D.-Y. Yang, S. H. Park, T. W. Lim, H. J. Kong, S. W. Yi, H. K. Yang, K.-S. Lee, *Appl. Phys. Lett.* **2007**, *90*, 013113.
[15] S. H. Park, S. H. Lee, D.-Y. Yang, H. J. Kong, K.-S. Lee, *Appl. Phys. Lett.* **2005**, *87*, 154108.
[16] R. H. Kim, J. S. Park, H. B. Sun, S. Kawata, K.-S. Lee, *Bull. Korean Chem. Soc.* **2008**, *29*(9), 1807.
[17] (a) D. A. Parthenopoulos, P. M. Rentzepis, *Science* **1989**, *245*, 843; (b) J. H. Strickler, W. W. Webb, *Opt. Lett.* **1991**, *16*, 1780; (c) K. D. Belfield, K. J. Schafer, *Chem. Mater.* **2002**, *14*, 3656; (d) A. S. Dvornikov, E. P. Walker, P. M. Rentzepis, *J. Phys. Chem.* **2009**, *113*, 13633. J. H. Strickler, W. W. Webb, *Opt. Commun.* **1991**, *16*, 1780.
[18] (a) J. D. Bhawalkar, N. D. Kumar, C. F. Zhao, P. N. Prasad, *J. Clin. Laser Med. Surg.* **1997**, *15*, 201, (b) S. Hirata, K.-S. Lee, T. Watanabe, *Adv. Funct. Mater.* **2008**, *18*, 2869; (c) H. M. Kim, M. J. An, J. H. Hong, B. H. Jeong, O. Kwon, J.-Y. Hyon, S.-C. Hong, K. J. Lee, B. R. Cho, *Angew. Chem. Int. Ed.* **2008**, *47*, 2231; (d) Y. Tian, W.-C. Wu, C.-Y. Chen, S.-H. Jang, M. Zhang, T. Strovas, J. Anderson, B. Cookson, Y. Li, D. Meldrum, W.-C. Chen, A. K.-Y. Jen, *J. Biomed. Mater. Res. A*, **2010**, *93A*, 1068.
[19] (a) J. B. Ehrlich, X.-L. Wu, I.-Y. S. Lee, Z. Y. Hu, H. Rockel, S. R. Marder, J. W. Perry, *Opt. Lett.* **1997**, *22*, 1843; (b) T.-C. Lin, G. S. He, Q. Zheng, P. N. Prasad, *J. Mater. Chem.* **2006**, *16*, 2490; (c) Q. Zheng, G. S. He, P. N. Prasad, *Chem. Phys. Lett.* **2009**, *475*, 250.
[20] (a) G. S. He, J. D. Bhawalkar, C. F. Zhao, P. N. Prasad, *IEEE J. Quantum Electron.* **1996**, *32*, 749; (b) G. S. He, R. Signorini, P. N. Prasad, *Appl. Opt.* **1998**, *37*, 5720; (c) E. Valle, S. Zippilli, F. P. Laussy, A. Gonzalez-Tudela, G. Morigi, C. Tejedor, *Phys. Rev. B*, **2010**, *81*, 035302.
[21] M. Albota, D. Beljonne, J.-L. Brédas, J. E. Ehrlich, J.-Y. Fu, A. A. Heikal, S. E. Hess, T. Kogej, M. D. Levin, S. R. Mader, D. McCord-Maughon, J. W. Perry, H. Rockel, M. Rumi, G. Subranmaim, W. W. Webb, X.-Y. Wu, C. Wu, *Science* **1998**, *281*, 1653.
[22] K.-S. Lee, M. S. Kim, H.-K. Yang, H. B. Sun, S. Kawata, P. Fleitz, *Mol. Cryst. Liq. Cryst.* **2004**, *424*, 35.
[23] S.-W. Kang, R.-H. Kim, J.-Y. Kim, Y. Iwase, K. Kamada, K.-S. Lee, *Nonlinear Opt., Quantum. Opt.* **2007**, *37*, 249.
[24] K.-S. Lee, H.-K. Yang, J.-H. Lee, O.-K. Kim, H. Y. Woo, H. Choi, M. Cha, M. Blanchard, *Desc. Proc. SPIE* **2003**, *4991*, 175.
[25] K.-S. Lee, J.-H. Lee, K.-S. Kim, H. Y. Woo, O.-K. Kim, H. Choi, M. Cha, G. S. He, J. Swiatkiewcz, P. N. Prasad, M.-A. Chung, S.-D. Jung, *Nonlinear Opt.* **2001**, *27*, 87.
[26] O.-K. Kim, K.-S. Lee, H. Y. Woo, K.-S. Kim, G. S. He, J. Swiatkiewcz, P. N. Prasad, *Chem. Mater.* **2000**, *12*, 284.
[27] J. Y. Kim, S.-W. Kang, K.-S. Lee, F. Hasegawa, T. Watanabe, *Nonlinear Opt., Quantum Opt.* **2005**, *34*, 175.

